Journal of Solid State Chemistry **144,** 118–124 (1999)
Article ID jssc.1999.8131, available online at http://www.idealibrary.com on IDEAL®

Gibbs Free Energy of Formation of $LnBa_2Cu_3O_{7-x}$ Phases Determined by the EMF Method (Ln = Yb, Tm, Er, Ho, Dy)

M. Kopyto and K. Fitzner

Institute of Metallurgy and Materials Science, Polish Academy of Sciences, 25 Reymonta Street, 30-059 Kraków, Poland

Received March 27, 1998; in revised form December 10, 1998; accepted December 23, 1998

Employing electrochemical cells with calcium fluoride solid electrolyte p_{O_2}, $CaO + CaF_2//CaF_2//CuO + LnBa_2Cu_3O_{7-x} + Ln_2CuBaO_5 + BaF_2$, p_{O_2}, for Ln = Yb, Er, Tm, Ho, Dy, and Gd, the Gibbs free energy change of the reaction of formation of the solid $LnBa_2Cu_3O_{7-x}$ phases for subsequent lanthanide elements was determined. Either an air or argon and oxygen gas mixture was used to fix oxygen potential over the reference and working electrodes. Next, the obtained results were used to derive the Gibbs free energy change of reactions of formation of the investigated $LnBa_2Cu_3O_{7-x}$ phases, except for that of the gadolinium compound. In this particular case, the side reaction made the reproducible cell performance impossible. © 1999 Academic Press

1. INTRODUCTION

The precise knowledge of phase equilibria and thermodynamic stability of respective oxide phases in terms of temperature and oxygen potential is required to define processing conditions of these materials. Unfortunately, except for a relatively large amount of information on the thermodynamic stability of phases existing in the Y–Ba–Cu–O system (1–3) gathered since the discovery of superconducting oxides, there is still virtually no data for similar compounds in quaternary systems with lanthanide elements.

This kind of thermodynamic information however may be very useful in modeling the liquid phase in any *Ln*–Ba–Cu–O system from known solubility data and Gibbs free energy of formation of respective compounds. Particularly, it may help to predict the solidifcation path by locating *solid* $Ln\langle 211\rangle$*–solid* $Ln\langle 123\rangle$*–liquid phase* conode, which in general is temperature and oxygen pressure dependent. In turn, this information is necessary for the successful crystal growth of $Ln\langle 123\rangle$ phases. A methodology, which couples the solidification process with the method of phase diagram calculations and kinetic models, is still being improved, and its details are given elsewhere (4–7).

Analyzing general trends in phase formation, solid solution formation, and phase relationships in these systems correlated with the size of the lanthanide Wong-Ng *et al.* (8) suggests that either gadolinium or europium changes the trend of the phase compatibility relations influencing the tie-line location in the CuO–BaO–Ln_2O_3 systems. Since the understanding of observed correlation between dimensions of the lanthanide ions, phase equilibria, and thermodynamic properties of respective phases still require new data concerning their thermodynamic properties, attempts have been made to enlarge thermodynamic information about these systems.

In the previous paper (9), we developed an experimental procedure based on the electrochemical cell with CaF_2 solid electrolyte, and we studied the stability of phases existing in the Eu–Ba–Cu–O system. We also reinvestigated Gibbs free energy of formation of double oxides in CuO–Ln_2O_3 systems for Ln = Yb, Tm, Er, Ho, Dy, and Gd (10). Next, using these data, the Gibbs free energy of formation of respective Ln_2CuBaO_5 phases (for Ln = Yb, Tm, Er, Ho, Dy, and Gd) was derived from our EMF measurements (11). In this work, we have determined the Gibbs free energy of formation of $LnBa_2Cu_3O_{7-x}$ phases for the same lanthanide elements using the EMF cell with a calcium fluoride electrolyte.

2. EXPERIMENTAL

a. Sample Preparation

Conventional ceramic methods were used to prepare Ln_2CuBaO_5 (designated as $Ln\langle 211\rangle$) phase and $LnBa_2Cu_3O_{7-x}$ phase (designated as $Ln\langle 123\rangle$) for Ln = Yb, Tm, Er, Ho, Dy, and Gd. Weighed amounts of powders of $BaCO_3$ (reagent grade) obtained from POCh, Gliwice (Poland) and CuO (99.999%) obtained from Johnson and Matthey (USA) were mixed with respective lanthanide oxides, palletized, and sintered under a stream of dry oxygen at about 1223 K. The Yb$\langle 123\rangle$ phase was synthesized under an argon and oxygen gas mixture with oxygen partial pressure reduced to 0.075 atm. Oxides of Ytterbium and Dysprosium were 99.9% pure and were

0022-4596/99 $30.00

both obtained from Unocal, Molycorp, Inc. (USA). Holmium oxide and Thulium oxide of the same purity 99.9% were obtained from Johnson and Matthey (Germany). Erbium oxide and Gadolinium oxide were 99.99% pure and were obtained from Rhone Poulenc (France). Single-crystal CaF_2 pellets used as solid electrolytes were obtained from Gimex (The Netherlands). The procedure of intermediate grinding, mixing, and palletizing was repeated three times.

The electrode pellets were prepared by mixing respective compounds with BaF_2 and were then sintered at 1173 K under a stream of dry oxygen, except for the compound with Yb. These electrodes were finally prepared under argon + oxygen gas mixtures. $CaO + CaF_2$ reference electrodes were made from equimolar amounts of the components in two steps. First, the pellets were sintered at 1273 K under argon for 24 h, and then after intermediate regrinding they were sintered again at 1173 K under dry oxygen for another 24 h.

b. Technique

The application of CaF_2-type electrolyte for thermodynamic study of oxide compounds has been discussed by Levitskii (12). The cell construction in this study was essentially identical with that described in our previous paper (11). The cell assembly used in our work is schematically shown in Fig. 1.

The cell was placed in a horizontal resistance furnace. The temperature was controlled by an Omega CN4821 temperature controller. The experimental temperature was measured with a Pt–PtRh10 thermocouple. Either dry, synthetics air (AGA, Sweden; virtually water-free) or argon and oxygen gas mixtures were flowed continuously through the cell vessel. The gas mixture was let into the cell through the electronic flowmeters obtained from Brooks Instrument (The Netherlands). This experimental setup permitted the EMF experiments to be run under a controlled oxygen partial pressure of 0.075 atm in the case of the Yb⟨123⟩ and

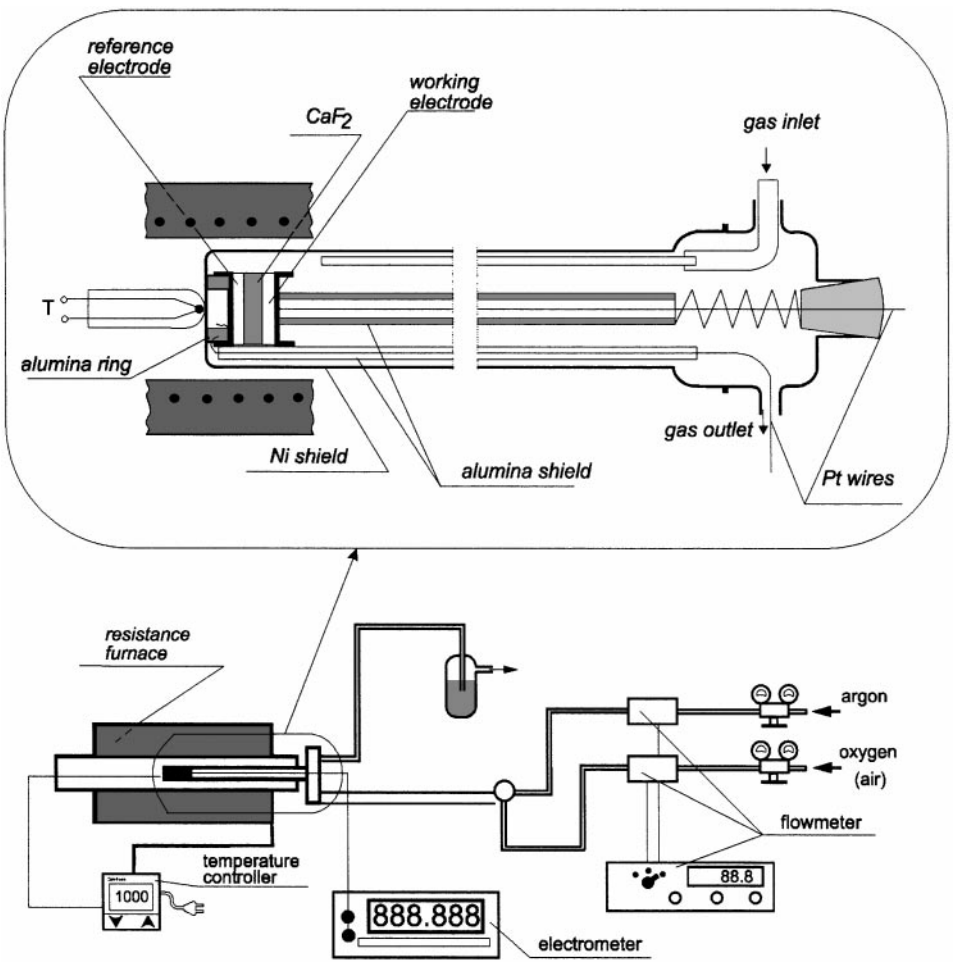

FIG. 1. Schematic diagram of the galvanic cell.

Tm⟨123⟩ phases. The EMF was measured with a Keithley 2000 electrometer. The equilibrium EMF values were attained in 3 to 10 h, depending on the temperature. The cell resistance was on the order of 10 kΩ in the temperature range from 973 to about 1100 K. The platinum lead wires did not show signs of reaction with the electrode pellets after the experiments. The EMF measurements were carried out in several cycles of increasing and decreasing temperature. Once the constant temperature had been reached, the EMF remained constant ($\pm$1–2 mV) for several hours until the temperature was changed again. Thermal cycling of the cell, under experimental conditions of repeated heating and cooling, produced virtually the same EMF values within the recorded scatter of points (shown for each cell in Fig. 2). Passing the current of 0.1 mA from the external source for 30 s also allowed the reversibility of the EMF to be checked. The EMF returned to the original values within $\pm$1 mV in about 1–5 min, depending on the temperature. All features of the cell performance mentioned above speak for the reversible cell behavior, although none of them give undeniable evidence of it. The whole experimental cycle of the cell operation usually took about one week.

3. RESULTS

The following electrochemical cells were assembled:

$$p_{O_2}, \mathrm{CuO} + Ln\langle 123\rangle + Ln\langle 211\rangle + \mathrm{BaF_2/CaF_2/CaO} + \mathrm{CaF_2}, p_{O_2} \qquad \mathrm{I}$$

for Ln = Yb, Tm, Er, Ho, Dy, and Gd.

The cell scheme is written in such a way that the right-hand electrode is positive. For galvanic cell I the electrode reactions are:

(a) at the RHS electrode

$$3\mathrm{CaF_2} + 3/2\mathrm{O_2} + 6\mathrm{e} = \mathrm{CaO} + 6\mathrm{F}^-. \qquad [1]$$

(b) at the LHS electrode

$$2Ln\mathrm{Ba_2Cu_3O_{7-x}} + 6\mathrm{F}^- = Ln_2\mathrm{BaCu_5} + 5\mathrm{CuO} + 3\mathrm{BaF_2} + (2-x)\mathrm{O_2} + 6\mathrm{e}. \qquad [2]$$

The overall cell I reaction is

$$3\mathrm{CaF_2} + 2Ln\mathrm{Ba_2Cu_3O_{7-x}} = 3\mathrm{CaO} + 5\mathrm{CuO} + 3\mathrm{BaF_2} + Ln_2\mathrm{BaCuO_5} + (0.5-x)\mathrm{O_2}. \qquad [3]$$

According to the available phase diagrams, the mutual solubility between solid phases (perhaps, with the exception of the Gd system) is small in the investigated temperature range. Consequently, all solid components of the reaction [3] are essentially in their standard state. Thus, for spontaneous reaction [3], the change in Gibbs free energy can be derived as

$$\Delta \mathrm{G} = -6FE_{\mathrm{I}} = \sum_i \nu_i \mu_i = \Delta \mathrm{G}^0_{[3]} + (0.5-x)\,\mathrm{RT}\ln p_{\mathrm{O_2}}, \qquad [4]$$

from where

$$\Delta \mathrm{G}^0_{[3]} = -6FE_{\mathrm{I}} - (0.5-x)\,\mathrm{RT}\ln p_{\mathrm{O_2}} \qquad [5]$$

can be calculated. In Eq. [5] E_{I} is the measured EMF (V) of the cell I, and $F = 96580\ \mathrm{J\ V^{-1}\ mol^{-1}}$ is the Faraday constant.

The variations of the EMF's with temperature determined for investigated systems are shown in Fig. 2.

All cells, except that with the Gd-phase, produced reproducible EMF values for about one week. The corresponding linear relations between EMF and temperature are given in Table 1 together with respective $-6FE_{\mathrm{I}}$ terms. Standard deviations as well as corresponding errors in $\Delta \mathrm{G}^0_{[3]}$ are also given in Table 1.

In our case, only the terms independent on $x(p_{O_2}, T)$ were calculated and are shown in Table 1 as $\Delta \mathrm{G}^0_{[3]} + (0.5-x)\mathrm{RT}\ln p_{\mathrm{O_2}}$, leaving the correction term to be evaluated for each particular system. This can be done only if the $p_{\mathrm{O_2}} - T - x$ dependence for respective $Ln\langle 123\rangle$ phase is known (e.g., from thermogravimetric measurements). Then, $\Delta \mathrm{G}^0_{[3]}$ can be calculated exactly from our EMF data under variable $p_{\mathrm{O_2}}$ conditions.

In the previous paper [9], we analyzed the literature data for the exchange reaction

$$\mathrm{CaO} + \mathrm{BaF_2} = \mathrm{CaF_2} + \mathrm{BaO} \qquad [6]$$

and have accepted the change in Gibbs free energy as given by Kaye and Laby (13), which is

$$\Delta \mathrm{G}^0_{[6]}(\pm 1000\ \mathrm{J}) = 63785 - 3.77 \cdot T. \qquad [7]$$

Combining reaction [6] with reaction [3] gives the reaction

$$2Ln\langle 123\rangle = Ln\langle 211\rangle + 5\mathrm{CuO} + 3\mathrm{BaO} + (0.5-x)\mathrm{O_2} \qquad [8]$$

Finally, using Gibbs free energy change of the reaction of formation of respective $Ln\langle 211\rangle$ phases from oxides determined in our previous work [11], one can derive the Gibbs free energy change of the reaction of formation of $Ln\langle 123\rangle$ phases from respective oxides by adding the reaction

$$Ln\langle 211\rangle = Ln_2\mathrm{O_3} + \mathrm{CuO} + \mathrm{BaO} \qquad [9]$$

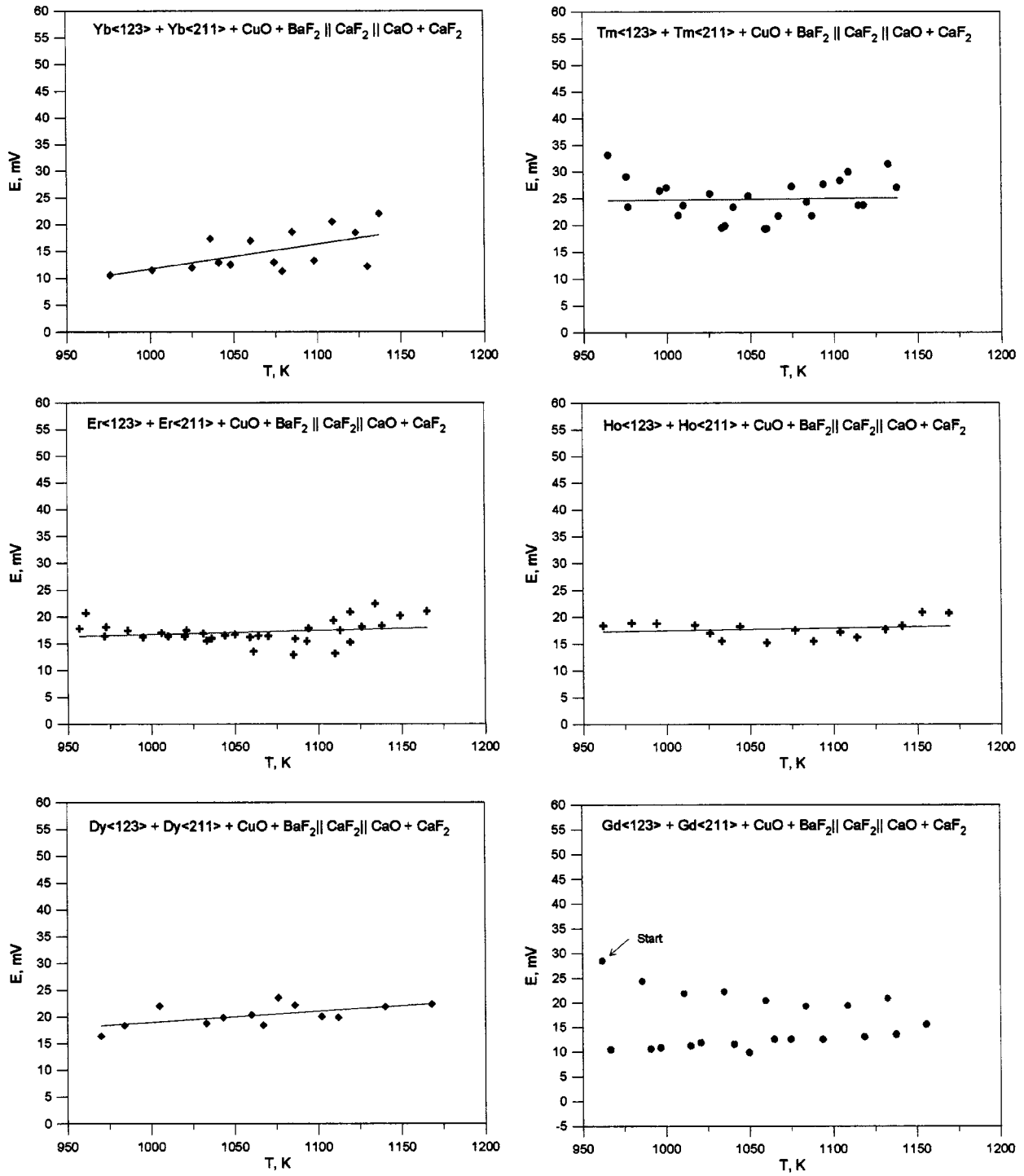

FIG. 2. Variation of EMF with temperature of cell I obtained for respective systems.

to reaction [8]. Thus, for the resulting reaction of formation from oxides and oxygen

$$1/2Ln_2O_3 + 2BaO + 3CuO + \{(0.5 - x)/2\}O_2 = Ln\langle 123\rangle. \quad [10]$$

Gibbs free energy of formation of one mole of $Ln\langle 123\rangle$ can be calculated. Consequently, obtained $\Delta G^0_{[10]} - \{(0.5 - x)/2\}RT\ln p_{O_2} = f(T)$ equations for subsequent $Ln\langle 123\rangle$ phases are shown in Table 1. Since these results are obtained by combining three reactions [3], [6], and [9],

TABLE 1
Observed EMF and Respective Gibbs Free Energy Change of the Reaction

Ln	$E_I = a + b \cdot T$ (mV)	$\Delta G^0_{[3]} + (0.5 - x) \cdot RT \cdot \ln(p_{O_2}) = -6FE_I$ $= A + B \cdot T$ (J/mol)	$\Delta G^0_{[10]} - (0.25 - \frac{1}{2}x) \cdot RT \cdot \ln(p_{O_2})$ $= A + B \cdot T$ (J/mol)
Yb[a]	$-34.56 + 0{,}0463 \cdot T$ ($\pm$ 3.12)	$20008 + 26.80 \cdot T$ ($\pm$ 5420)	$-133184 + 16.63 \cdot T$ ($\pm$ 6800)
Tm	$21.90 + 0.0028 \cdot T$ ($\pm$ 3.87)	$-12678 - 1.62 \cdot T$ ($\pm$ 6720)	$-115143 + 3.96 \cdot T$ ($\pm$ 7620)
Er	$9.14 + 0.0076 \cdot T$ ($\pm$ 2.17)	$-5291 - 4.38 \cdot T$ ($\pm$ 3770)	$-122728 + 7.01 \cdot T$ ($\pm$ 5140)
Ho	$12.61 + 0.0048 \cdot T$ ($\pm$ 1.71)	$-7300 - 2.80 \cdot T$ ($\pm$ 2970)	$-118424 + 3.23 \cdot T$ ($\pm$ 4520)
Dy	$-1.79 + 0.0208 \cdot T$ ($\pm$ 1.68)	$1033 - 12.02 \cdot T$ ($\pm$ 2920)	$-121883 + 7.13 \cdot T$ ($\pm$ 4460)

[a] $p_{O_2} = 0.075$ atm.

errors in $\Delta G^0_{[10]}$ shown in Table 1 were calculated using the formula

$$\sqrt{(\delta\Delta G_{[3]})^2 + (3^*\delta\Delta G_{[6]})^2} + (2^*(\Delta(G)_{[9]})^2.$$

Because of the fact that oxygen partial pressure in air (0.21 atm) and in an oxygen + argon gas mixture (0.075 atm) was kept constant during the experiments, only the dependence $x = f(T)$ under these conditions is required to calculate the correction term. This procedure is demonstrated in the Discussion section using experimental data reported recently by Ishizuka *et al.* (14) for the Dy$\langle 123 \rangle$ phase.

4. DISCUSSION

Our results obtained for respective *Ln*$\langle 123 \rangle$ phases are shown in Table 1. Since the correction term $\{(0.5 - x)/2\}$ RT ln p_{O_2} was not determined experimentally in this work, final results shown in the table correspond to the Gibbs free energy of formation of respective phases from oxides, i.e., for $x = 0.5$. Obtained enthalpies of formation however are independent on this correction term and they can be compared directly with other available literature data.

Zhou and Navrotsky (15) found that the enthalpy of formation of Y$\langle 123 \rangle$ depends on oxygen content, $(7 - x)$. According to their study it varies with x from -74.2 for the oxygen deficient phase $YBa_2Cu_3O_6$ to -106.2 kJ/mole for the oxygen saturated phase $YBa_2Cu_3O_7$. Morss *et al.* (16) reported the enthalpy value -126.0 kJ/mole for the oxygen saturated compound at room temperature.

Corresponding enthalpy values derived from EMF measurements for the Y$\langle 123 \rangle$ phase vary from -53.0 (17) through -109.0 (18) to -210 kJ/mole (19). Our estimated enthalpy value for the Eu$\langle 123 \rangle$ phase falls in the similar ballpark: -163.3 kJ/mole (9). Recently, Lamberti *et al.* (20) performed thermochemical investigations of compounds with *Ln* = Pr, Nd, Eu, Gd, Dy, Ho, and Tm and found that the enthalpies of formation of *Ln*$\langle 123 \rangle$ phases display essentially linear trend toward less exothermic values with increasing lanthanide atomic number, i.e., decreasing ionic radius. These results indicate that phases with larger lanthanide ions may be more stable.

In Fig. 3 we compared the available enthalpy values as a function of trivalent ionic radius of rare earth ion. The presented plot indicates good agreement between calorimetric results and our values derived from EMF measurements. Also, a general trend in the enthalpy of formation from oxides with the change of ionic radius of the lanthanide element along the row of the periodic table shown in Fig. 3 is compatible with conclusions of the work (20).

As the size of the lanthanide ion increases, the unit cell volume increases. This change is accompanied with a decrease of orthorombic distortion defined as a difference of the lattice parameters *a*–*b*, At the same time, a slight increase of the critical temperature, T_c, with increasing ionic radius is observed (21). It is interesting to note that although the measured enthalpy value for the Pr$\langle 123 \rangle$ follows the general trend depicted in Fig. 3, this phase is not superconducting, and its orthorombic distortion suddenly increases in comparison with other phases.

Results gathered in Table 1 also suggest that all *Ln*$\langle 123 \rangle$ phases are not entropy stabilized, though the entropy term is influenced by the oxygen stoichiometry of the respective phase. This term yields a much smaller contribution to Gibbs free energy than the corresponding enthalpy term.

All EMF cells with lanthanide elements but Gd worked reversibly. The change of EMF with temperature recorded for this cell is shown in Fig. 2. An X-ray study of the working electrode performed after the experiments showed the formation of a $BaF_2 \cdot GdF_3$ compound. It is also possible that the solid solution range into which Gd$\langle 123 \rangle$ may extend (8) is wider. In this case, however, we could not choose another three-phase equilibrium field to retard side reaction, in a way we had done that with Gd$\langle 211 \rangle$ (11). That is why we are forced to conclude that Gibbs free energy of formation of the Gd$\langle 123 \rangle$ phase cannot be determined with the EMF cell of the type I.

It is worth mentioning that we encountered some difficulties while working with the Yb$\langle 123 \rangle$ phase. It appeared it could not be synthesized by conventional techniques of

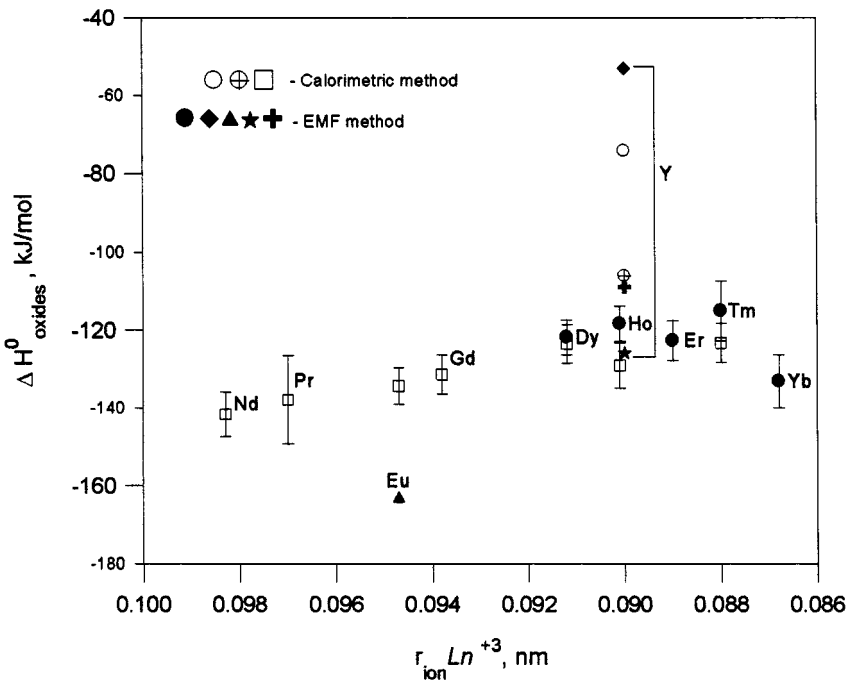

FIG. 3. Standard enthalpy of formation of $Ln\langle 123\rangle$ phases from oxides vs trivalent ionic radius of rare ion. (○) Zhou and Navrotsky (15) $x = 1$; (⊗) Zhou and Navrotsky (15) $x = 0$; (□) Lamberti *et al.* (20); (◆) Pashin and Tretyakov (17); (▲) Przybyło *et al.* (9) (★) Morss *et al.* (16); (+) Fan Zhanguo *et al.* (18); (●) this work.

phase preparation. The explanation of this fact came with the work of Osamura and Zhang (22) who showed that the stable region of the Yb$\langle 123\rangle$ phase extends below 0.1 atm. Consequently, it can be made under neither oxygen nor air at high temperature. Having this information we successfully synthesized the Yb$\langle 123\rangle$ phase under reduced oxygen pressure (0.075 atm) using an argon + oxygen gas mixture, and we ran EMF experiments under the same conditions.

Finally, one should consider the influence of oxygen nonstoichiometry on the free energy of formation of the $Ln\langle 123\rangle$ phases. The best solution of this problem could be a universal model, which yields $x(T)$ for fixed oxygen pressure for chosen lanthanide phase. This however seems unlikely, mainly due to the discrepancy between experimental data obtained for different systems with a different experimental approach. Thus, it may not be a bad idea to demonstrate how oxygen nonstoichiometry can influence $\Delta G^0_{f,\,oxides}$ derived from our study for one system. Apart from individual differences, the $x - T - p_{O_2}$ dependence should exhibit the same character for all phases independently on the lanthanide element. Consequently, the general pattern in Gibbs free energy change under the influence of oxygen nonstoichiometry of the phase should also be similar.

Recently, Fueki *et al.* (14) reported the $x - T - p_{O_2}$ dependence for the Dy$\langle 123\rangle$ phase. We used their following data: 673 K, $x = 0.1016$; 773 K, $x = 0.2008$; 873 K, $x = 0.3435$; 973 K, $x = 0.4694$; 1073 K, $x = 0.5782$; 1173 K, $x = 6580$ to calculate the correction term in ΔG^0 equation. Gibbs free energy change for reaction [10] in this case can be expressed as

$$\Delta G^0_{[10]} = \Delta G^0_{f,\,oxides} + \{(0.5 - x)/2\} RT \ln p_{O_2}. \quad [11]$$

Gibbs free energy change of reaction [10] for $x = 0.5$ is simply equal to Gibbs free energy change of the reaction of formation of the Dy$\langle 123\rangle$ phase from respective oxides. The term $\{(0.5 - x)/2\}\ RT \ln p_{O_2}$ takes into account a deviation of the oxygen content from $x = 0.5$ and can be determined from the experimental data given above. Using the data from Table 1, Eq. [11] can be rewritten in the form

$$\Delta G^0_{[10]} = -121795 + 3.93 \cdot T - x(p_{O_2} = 0.21, T) * 6.49 \cdot T \text{ J/mole}. \quad [12]$$

The results of our calculations are shown in Fig. 4, in which the broken line represents Gibbs free energy change of the reaction [10] of formation of the Dy$\langle 123\rangle$ phase from oxides (i.e., for $x = 0.5$). The solid line shows the results of calculations if oxygen nonstoichiometry of the phase for fixed oxygen partial pressure ($p_{O_2} = 0.21$ atm) is taken into account. It can be seen from this figure that at low temperature oxygen excess results in additional phase stabilization, thereby lowering the Gibbs free energy of the reaction of the

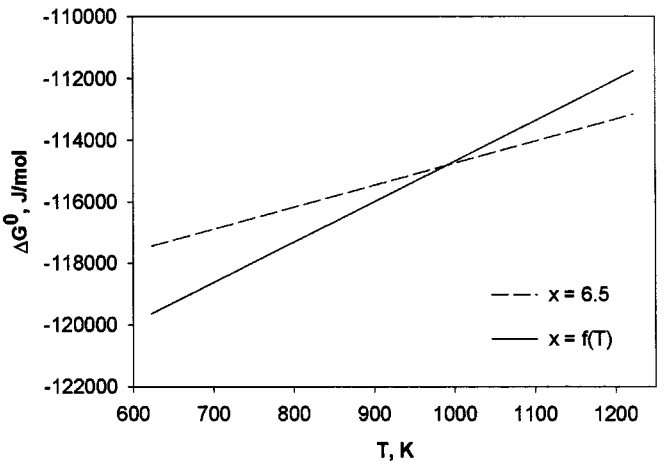

FIG. 4. Gibbs free energy change of the reaction [10] as a function of temperature and oxygen content of the Dy⟨123⟩ phase.

phase formation. In turn, at high temperature, oxygen deficiency makes the Gibbs free energy for the same reaction more positive, additionally destabilizing the phase. It seems that apart from individual differences this picture should be generally obeyed for all *Ln*⟨123⟩ phases.

Now, further measurements should be carried out to find out how these findings apply to systems with Samarium and Neodymium, where phase relations are different.

ACKNOWLEDGMENT

This work was supported by the State Committee for Scientific Research under Grant 7T08D 008 09.

REFERENCES

1. T. B. Lindemer, J. F. Hurley, J. E. Gates, A. L. Sutton, J. Brynestad, C. R. Hubbard, and P. K. Gallagher, *J. Am. Ceram. Soc.* **72,** 1775 (1989).
2. G. F. Voronin and S. A. Degterov, *Physica C* **176,** 387 (1991).
3. J. Sestak, *Pure Appl. Chem.* **64,** 125 (1992).
4. W. A. Tiller, "The Science of Crystallization." Cambridge University Press, Cambridge, UK (1991).
5. S. W. Chen, Y. Y. Chuang, and Y. A. Chang, *Met. Trans. A* **22A,** 2837 (1991).
6. T. Kraft and Y. A. Chang, *JOM* **20** (1997).
7. Ch. Krauns, Ph.D. thesis, University of Göttingen (1995).
8. W. Wong-Ng, B. Paretzkin, and E. R. Fuller, *J. Solid State Chem.* **85,** 117 (1990).
9. W. Przybyło, B. Onderka, and K. Fitzner, *J. Solid State Chem.* **126,** 38 (1996).
10. M. Kopyto and K. Fitzner, *J. Mater. Sci.* **31,** 2797 (1996).
11. M. Kopyto and K. Fitzner, *J. Solid State Chem.* **134,** 85 (1997).
12. V. A. Levitskii, *Vestn. Moskov. Univ. Ser. Chimia*, **19(2),** 107(1978).
13. G. W. C. Kaye and T. H. Laby, "Tables of Physical and Chemical Constants." Longmans, London (1966).
14. H. Ishizuka, Y. Idemoto, and K. Fueki, *Physica C* **195,** 145 (1995).
15. Z. Zhou and A. Navrotsky, *J. Mater. Res.* **7,** 2920 (1992).
16. L. R. Morss, S. E. Dorris, T. B. Lindemer, and N. Naito, *Eur. J. Solid State Inorg. Chem.* **27,** 1327 (1990).
17. S. F. Pashin and Yu. D. Tretyakov, *in* "Chemistry of High Temperature Superconductors" (C. N. R. Rao, Ed.), p. 306. World Scientific, Singapore (1991).
18. Fan Zhanguo, Ji Chunlin and Zhao Zhongxiang, *J. Less-Common Met.* **161,** 49 (1990).
19. A. M. Azad, O. M. Sreedharan, and K. T. Jacob, "International Conference on High Temperature Superconductors," Bangalore, India, Jan. 1990.
20. V. E. Lamberti, M. A. Rodriguez, J. D. Trybulski, A. Navrotsky, and H. B. Liu, *Chem Mater.* **9,** 932 (1997).
21. B. Raveau, C. Michael, M. Hervieu, and D. Groult, "Crystal Chemistry of High-T_c Superconducting Copper Oxides." Springer-Verlag, Berlin/New York (1991).
22. K. Osamura and W. Zhang, *Z. Metallkd.* **84,** 522 (1993).